XMaS

the UK-CRG

NEWSLETTER

2004

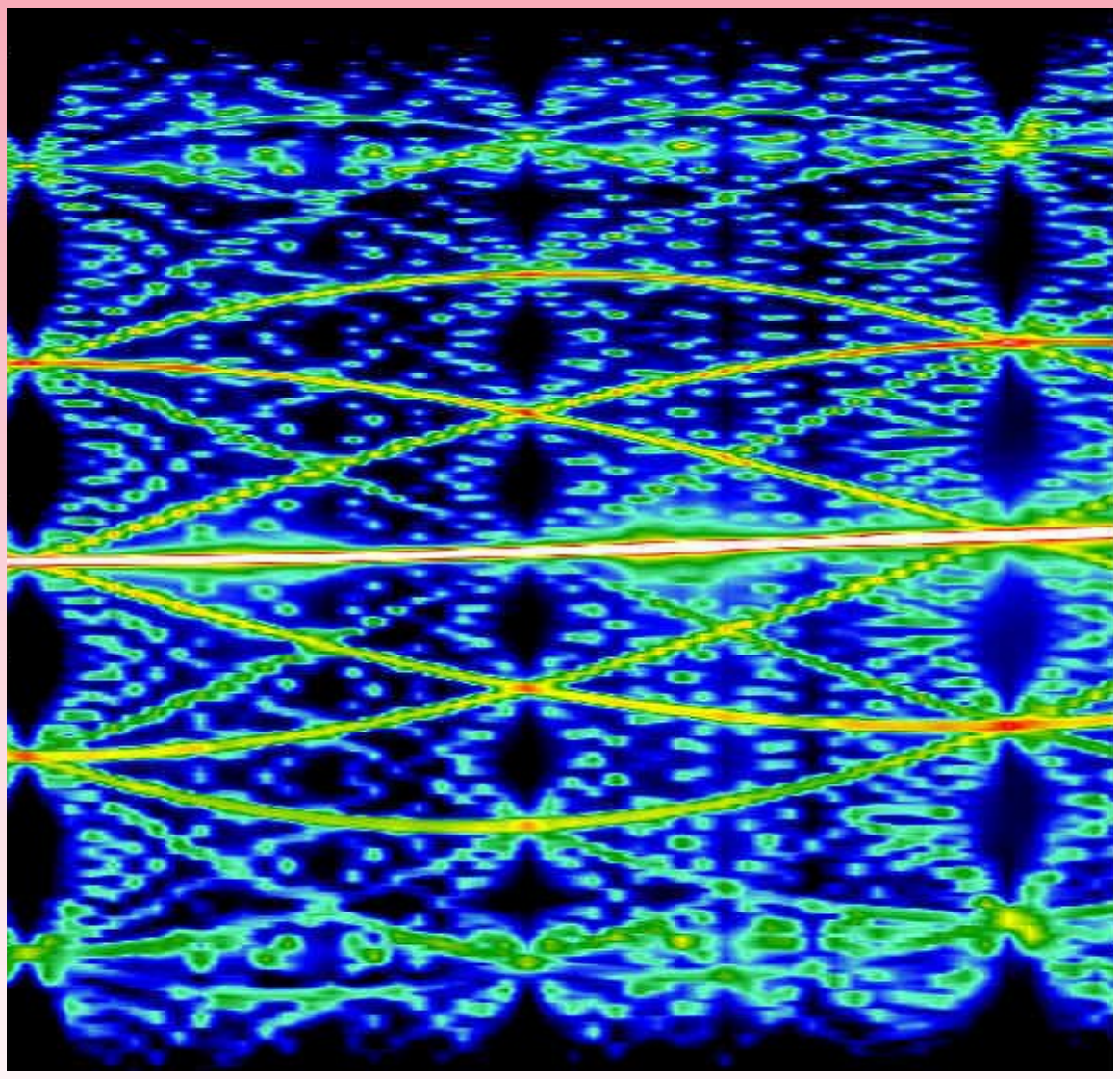

Contents

Status

During 2004 the beamline has operated without major problems and the MAR detector has been brought into regular use. We await with baited breath the arrival of the 4T magnet and the tailor-made cryostat with a suitably slimmed down tail. Commissioning of these major items is scheduled for March 2005 with user experiments scheduled for later in that cycle.

The three stage closed cycle refrigerator operating with ^{3}He is available for routine use and offers the possibility of a base temperature of 1.0K.

One notable development has been the modification of the monochromator mount to extend the usable energy range down to 2.4 keV. This is described under instrumental developments and the potential to study effects at the sulphur edge (2.5keV) is discussed in the short article by Bob Cernik that follows the description.

Also under instrument developments is a description of the development of a diamond phase plate flipper. This will offer the ability to flip the helicity of the x-ray beam as an alternative to flipping the magnetic field. This can be done far more rapidly than field flipping, the more so where experiments are anticipated involving the 4T magnet.

The recabling work in the experimental hutch and control cabin, mentioned in the 2003 Newsletter, was completed and the anticipated reduction in detector noise has been fulfilled. Where we were suffering background counts of several/second we are now experiencing improvements of two orders of magnitude.

Cover illustration: Grazing incidence scattering showing the in-plane diffraction pattern from an array of nanoscale dots of $Ni_{60}Fe_{40}$ alloy on a square lattice with a periodicity of 1.25microns. The data was recorded at a scattering angle of 1.5° as the sample was rotated about the surface normal. Courtesy: TPA Hase, D Atkinson and BK Tanner, et al, Physics Department, Durham University.

User meeting held in March at Liverpool University

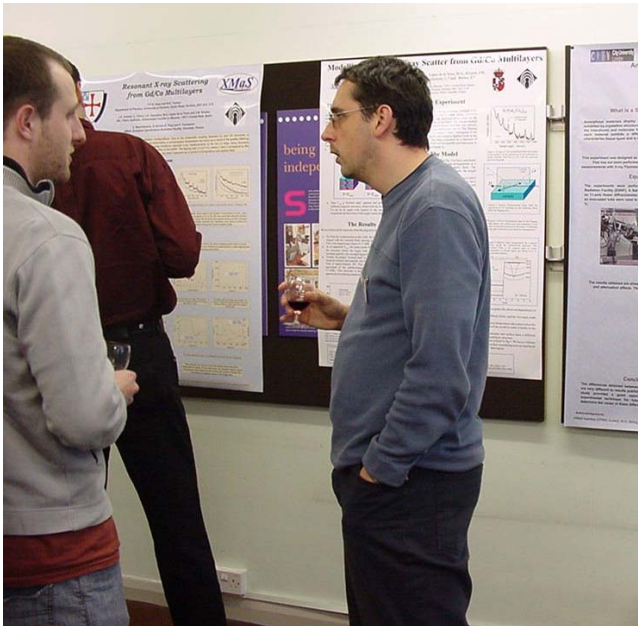

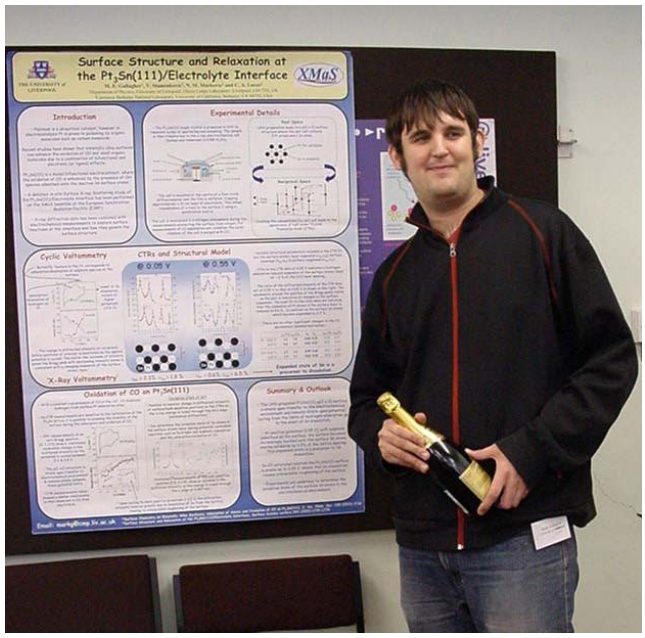

The two pictures above were taken during the poster session at the end of the meeting. The picture on the right shows the poster competion winner, Mark Gallagher, holding his prize in front of the winning presentation.

Instrumental Developments

Extending the Energy Range

The beamline specification, finalised 10 years ago during the design phase, set the energy range of the beamline, with silicon 111 crystals installed, to be 3—15 keV. Nevertheless, it has been found possible to perform experiments at energies somewhat outside this range. Recently, an experiment at the sulphur K edge (2.47 keV) became of interest and an investigation was conducted to determine the actual low energy cutoff of the monochromator. This was found to be ~ 2.7 keV. However, it was quickly established that a simple modification to the first crystal support would allow an extension to include the sulphur K edge. Figure 1 shows the new modified support, now with increased angular relief, allowing higher angle (lower energy) beams to pass unimpeded through the crystal assembly. Figure 2 shows an energy plot, taken following the modification, demonstrating access to energies >2.4 keV. The contribution from R. Cernik overleaf illustrates further possibilities for experiments at this energy.

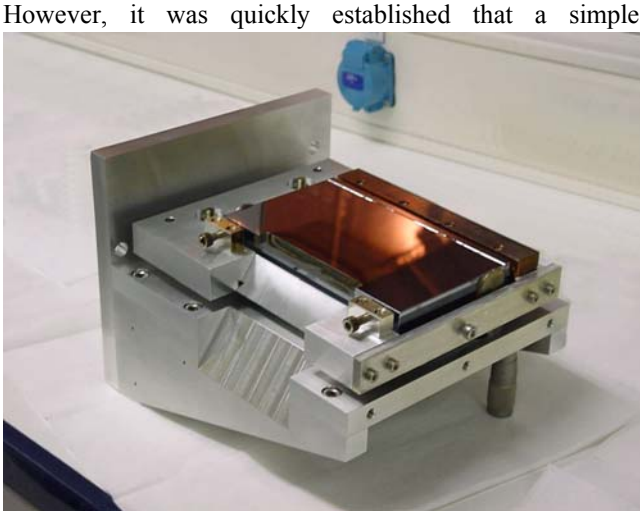

Figure 1: New first crystal mounting.

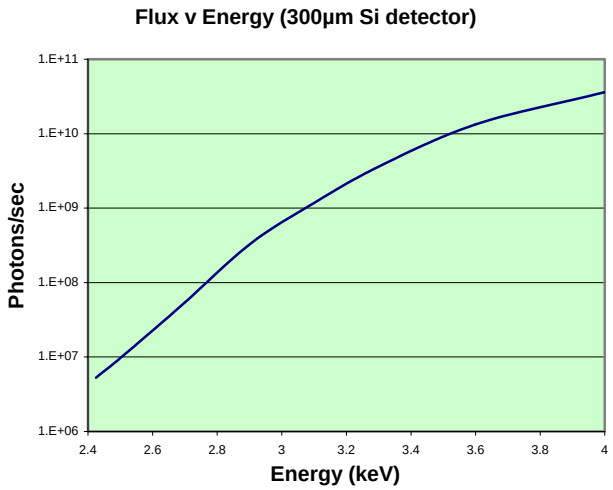

Figure 2: This plot is corrected for absorption within the Si of the detector.

Softer x-ray resonant scattering

R J Cernik, CCLRC Daresbury Laboratory, Daresbury, Warrington, WA4 4AD, UK—for further information contact r.j.cernik@dl.ac.uk

The news that XMaS can now operate at x-ray energies down to 2.5keV opens up a number of possibilities for new experiments. This account describes a Daresbury study of the sulphur-containing drug promazine hydrochloride, $C_{17}H_{21}N_2SCl$.

There are many occasions in materials science where a detailed understanding of the crystal structure assists the design process. We were therefore interested to see whether we could use the sulphur atoms present in the material to solve the crystal structure of a number of industrially important pharmaceutical polymorphs. Specifically, construction of a difference Patterson map corresponding to diffraction patterns collected on- and off- the sulphur edge allows us to simplify the Patterson map significantly. Indeed, when there is only one sulphur atom in the asymmetric unit of a centro-symmetric triclinic structure, the difference Patterson map essentially corresponds to the crystal structure itself.

Measurements at 2.35keV ($f' = -3.38$; $f'' = -0.44$) and 2.44keV ($f' = -7.68$; $f'' = -0.41$) produces sufficient discrimination to give a strong effect for the anomalous signal in the Patterson difference map. The success of this approach has general implications for materials research as an analytical tool. For example, in the manufacture of microporous catalysts, knowledge of the structure surrounding cations in alumino-phosphates requires a better structural definition than can be provided by conventional X-ray crystallography.

We used station 3.4 on the SRS at Daresbury in order to access the anomalous scattering from sulphur in a sample of promazine hydrochloride. In order to work close to the sulphur absorption edge at 2.472 keV we used an in-vacuum diffractometer, borrowed from the experimental systems group at Daresbury. This vacuum vessel had previously been used for testing optical elements, gratings, monochromator elements and for soft x-ray magnetic studies of single crystals and has been used at the ESRF on a number of occasions. The diffractometer was not optimised for our powder samples.

The diffraction signal was weak but observable. This is shown in Figure 1 with three traces from promazine hydrochloride 4eV, 10 eV and 200 eV below the sulphur edge. The data were collected at a constant angle (ω) with respect to the incident beam. The angle ω was then altered and a repeat scan was made. This was instead of sample rotation or rocking since the design of the diffractometer prevented either movement. The penetration depth at 2.4 keV with an average incidence angle of 7 degrees is only one to two microns. The number of powder grains in the diffracting position is therefore limited. In addition the method is highly sensitive to those grains lying on the surface of the material. Despite these difficulties we collected many data sets at slightly different ω values and averaged them together: a time consuming process! The resulting data fit a LeBail refinement (Figure 2) with a quadrupled unit cell from the published value in the *b* direction and a distorted triclinic cell compared with the published structure. The peak half widths are of the order of 0.2 degrees. This is what we expect since the rocking width of the sample is ~ λ^2. The nature of the peak splitting is still not understood.

A purpose built diffractometer for softer X-ray work, with an integral area detector, needs to be constructed for further studies. We have designed a simple soft X-ray powder diffractometer working in a low vacuum system that will be ideal for these experiments.

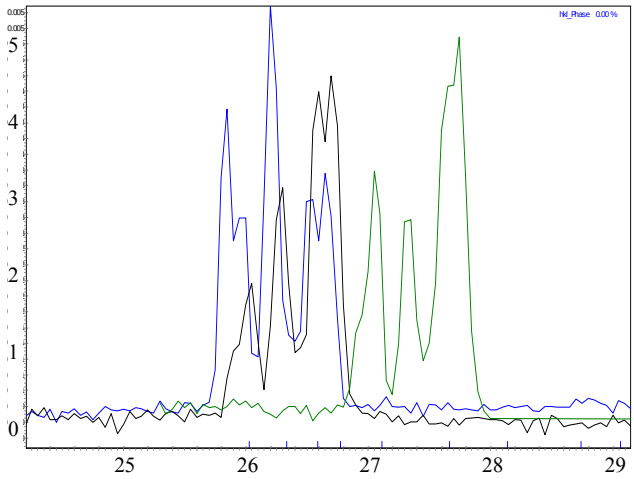

Figure 1: Promazine hydrochloride close to the sulphur edge, 4 eV below (blue), 10 ev below (Black), 200 eV below (green)

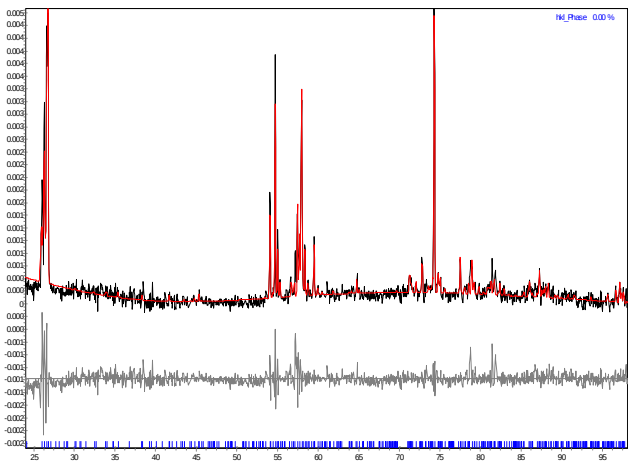

Figure 2: A Le Bail refinement of the unit cell at 2.3 keV

Diamond phase-plate flipper

A diamond phase-plate is used to produce either circular polarisation, as in reflectivity or XMCD measurements, or elliptical polarisation, employed in non-resonant x-ray diffraction experiments, for which the polarisation factor, $P_C/(1-P_L)$, is maximised. The phase plate is often used in combination with a magnetic field, applied to the sample, and frequently, where the "flipping ratio" is of interest, the field is reversed cyclically. Not without success, results are often limited by factors, such as, sample heating from the field reversal and inherent slowness in the field cycling causing beam instability to be an issue. There are additional problems for samples that are either hard magnets, are strongly magnetostrictive, or are soft-materials having some field history dependence. This has prompted the development of a method for reversing the polarisation of the x-ray beam rather than switching the direction of the external magnetic field, since this has the potential for significantly higher switching speeds. This approach should be even more important for experiments using the 4T Magnet, soon to be commissioned on the beamline, where it is envisaged that field switching times will be orders of magnitude longer than those for the 1T magnet! Thus, reversing the helicity will improve the signal to noise ratio, be less time consuming and produce data less affected by beam movements.

Because of the different angular motions required of the diamond crystal, <250 arcsec for circular polarisation and <1.5 deg. for elliptical, it is forseen that two different actuator systems will be employed. For the former, the motion will be based on a piezo-actuator with absolute positioning controlled by a lock-in device that will reduce the signal to noise ratio and thereby allow the measurement of very small signals (10^{-4}-10^{-6}). Switching frequencies of 5 → 40 Hz for the helicity of beam are anticipated. The design principle adopted for the stage is similar to that in use at the 4-ID-D beamline at the APS (Figure 1) but will be miniaturised in order to fulfil the beamline space constraints. The motion for the elliptical polarisation, probably based on a mechanical system, will allow operation at similar frequencies.

The design study is being undertaken by the NPL's Functional Materials Group, which, not only has 12 years experience in the characterisation of electroactive materials such as piezoelectric ceramics, but also are well experienced in instrument design and industry-based materials metrology. The detailed design drawings for the prototype are scheduled for the early summer.

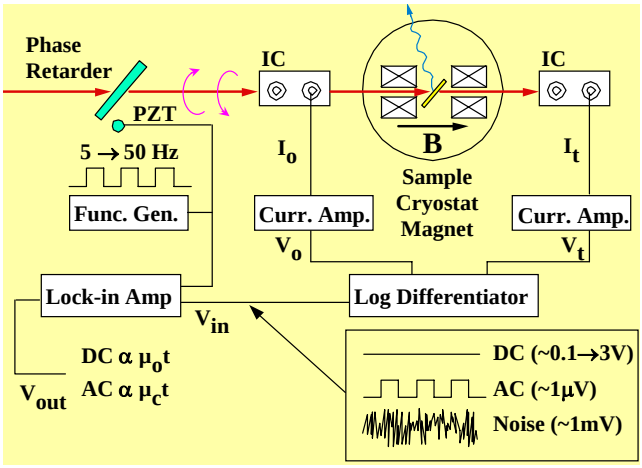

Figure 1: Schematic of phase lock setup used at the 4-ID-D beamline at the APS.

Search for Γ_5 Octupole order in $Ce_{0.7}La_{0.3}B_6$

D. Mannix, Y. Tanaka, S. Lovesey, K. Katsumata, G. Carbone, N. Bernhoeft and S. Kuni—for further information contact D. Mannix at XMaS, BM28, ESRF danny@esrf.fr

CeB_6 and its substitutional solid solution $Ce_xLa_{1-x}B_6$ are celebrated Kondo materials with space group *Pm3m*. Several competing ground states condense out of the paramagnetic phase (phase I), under bias of temperature, applied magnetic field and La doping concentration. In the pure CeB_6 compound, the primary order parameter below $T_Q = 3.2$K is described by an antiferro-type motif of electric quadrupole (so-called antiferroquadrupole AFQ order). However, dipole antiferromagnetic (AFM) coupling occurs below $T_N = 2.4$K (phase III) and become the primary order parameter under the application magnetic fields. The substitution of La ions radically changes the phase diagram and gives rise to a recently proposed and unknown new phase (phase IV), that is prominent in $Ce_xLa_{1-x}B_6$ at x~0.7 below $T_{I\text{-}IV} = 1.4$K. The evidence for a new phase comes from the incompatibility of several experiment results. A cusp in the magnetic susceptibility, characteristic of AFM order, is observed below $T_{I\text{-}IV}$ and similar to that found below $T_N = 3.2$K in the pure CeB_6. However, no evidence for long range magnetic order can be detected from neutron diffraction or muon spin rotation experiments. Furthermore, there is a large softening in the C_{44} elastic constant, that is not observed in the phase II AFQ state of pure CeB_6 and is inconsistent with an AFQ

order parameter in phase IV. These convincing arguments for a new phase have led to the postulation of a Γ_{5u} magnetic octupole ground state in phase IV. No direct evidence of magnetic octupole order has been reported, but in principle it can be probed by resonant x-ray magnetic scattering (RXMS) via electric quadrupole (E2) transitions that probe the 4*f* states. This requisite can be satisfied at the $L_{2,3}$ absorption edges of the rare-earths.

The aim of this work has been to investigate phase IV in $Ce_{0.7}La_{0.3}B_6$ using RXS for the first time, to search for signatures of Γ_{5u} octupole order by E2 RXMS. The XMaS beamline provides an impressive sample environment towards this end with the new ^{3}He Joule-Thomson cryostat. The cryostat is compact enough to be mounted for azimuthal scans, it fits inside the current XMaS 1-Tesla electro-magnet and provides a base temperature of 1-Kelvin. Using this setup, a double energy RXS response was observed in the vicinity of the Ce L_2 absorption edge (Figure 1) at the forbidden (½ ½ ½) Bragg position. Judging from the location of the white line in the fluorescence spectrum, the higher energy peak maybe attributed to E1 transitions that probe the Ce 5*d* conduction band, while the lower energy peak to E2 transitions to the 4*f* states. The temperature dependence of the E2 RXS intensity is shown in Figure 2 and disappears at about 1.4K, in agreement with $T_{I\text{-}IV}$ derived from other forgoing experiments. We have also investigated the azimuthal dependence at 1-Kelvin of the E2 RXS, which is shown in Figure 3. The six-fold azimuthal symmetry we observe (without polarisation analysis of the scattered beam) is not consistent with either AFQ or AFM order parameters. The azimuthal dependence maybe consistent with either magnetic octupole order or electric hexadecapole order. We are currently developing a theoretical model to account for the azimuthal dependence of the RXS and further work is planned on this material using polarisation analysis which will help determine the order parameter in phase IV.

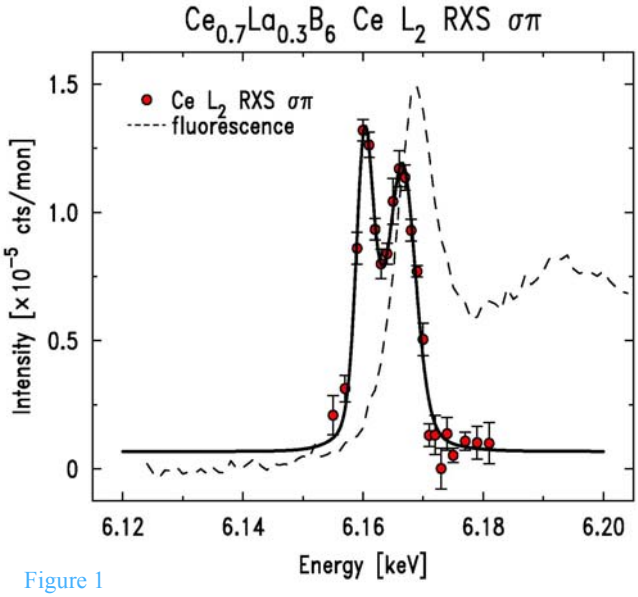

Figure 1

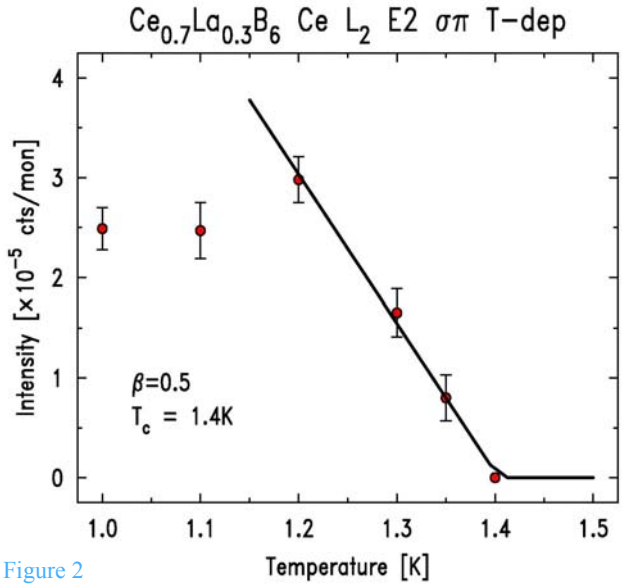

Figure 2

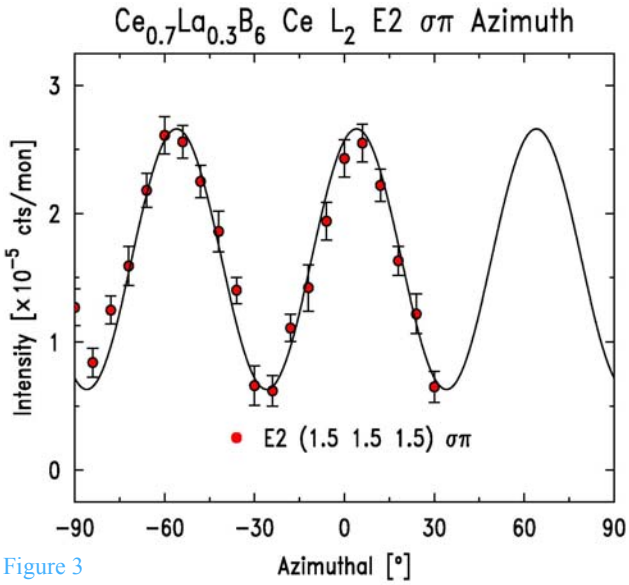

Figure 3

RXMS in $NpAs_{1-x}Se_x$ Solid Solutions

V.H.N. Rodrigues, J.A. Paixão, M.M.R. Costa, A. Bombardi, S. Wilkins, D. Mannix, J. Rebizant and G.H. Lander - for further information contact J.A. Paixão at Physics Department, University of Coimbra, P-3004-516 Coimbra, Portugal jap@pollux.fis.uc.pt

$NpAs_{1-x}Se_x$ solid solutions exhibit an interesting magnetic phase diagram. As the concentration of *p*-electrons increases with increasing Se content, the triple-k magnetic structure of NpAs changes into a non-collinear ferrimagnetic structure where both ferro and antiferro components coexist at low temperature.

We have recently performed the first experiment with transuranium elements at the XMaS beamline, using x-ray resonant scattering (RXS), to study two samples of $NpAs_{1-x}Se_x$ with compositions x = 5% and 10%. Most of the data was collected at the M_{IV} absorption edge of the actinide (3.846 keV) with a Au (111) crystal used for polarisation analysis.

Overall, there is good agreement between the magnetic phase diagram determined from neutron-scattering and our measurements. Our data unambiguously determined that the incommensurate phase occurring before the onset of ferromagnetism is single-k and confirmed that the mixed phase at low-T is ferrimagnetic, with both ferro and antiferromagnetic components coexisting in a single crystal grain. Moreover, a high resolution measurement of magnetostriction at high energy using a Si(444) analyzer clearly shows an orthorhombic lattice distortion taking place at T_C= 128 K, which agrees with the model suggested from the neutron data.

A new result was obtained in this experiment, the observation of resonant magnetic scattering from a ferromagnetic moment. The resonant magnetic scattering at the M_{IV} edge of the actinide is large enough to be separated from the charge scattering by simple polarisation analysis selecting photons with rotated polarization (Figure 3). The large signal (~2000 ct/s) could easily be followed as function of temperature down to the Curie temperature of 150 K as shown in Figure 4. This result enlarges the scope of RXMS into the field of ferro and ferrimagnets in samples with strong magnetic resonances.

Finally, a small resonant signal was also measured at antiferromagnetic reflections in the rotated polarisation channel when the energy was tuned to the As K-edge. This has also been observed in the isostructural $UAs_{1-x}Se_x$ system, but the resonance observed in the Np compound is not as large. This effect may be due to hybridisation between the actinide 5f electrons and the p-electron band, which is probably smaller in the $NpAs_{1-x}Se_x$ system.

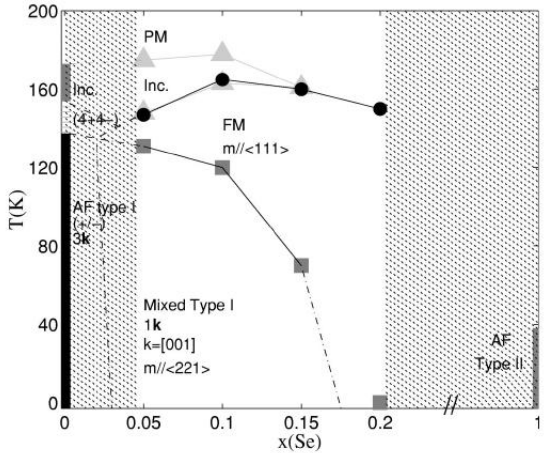

Figure 1: Phase diagram of $NpAs_{1-x}Se_x$ in zero field [2]. The shaded areas correspond to unexplored regions of the phase diagram.

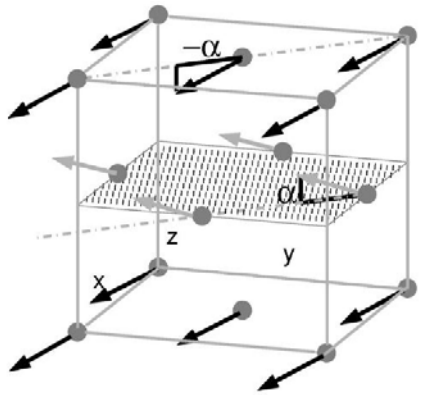

Figure 2: Magnetic structure at low T in $NpAs_{1-x}Se_x$ in the mixed type I phase proposed by Bombardi et al. [2] from neutron and magnetization data. In the domain shown a FM component along [110] is superimposed with an AF component along [001] so that the magnetic moments are tilted by an angle a (~18º) with respect to the [110] axis.

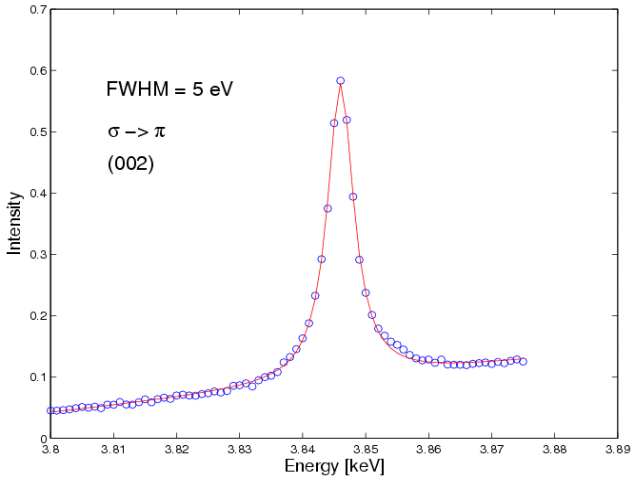

Figure 3: Energy scan through the Np M_{IV} edge of the (002) reflection on the rotated channel, showing the large resonance below the ferromagnetic ordering temperature (data taken at 8 K on the $NpAs_{0.90}Se_{0.10}$ sample).

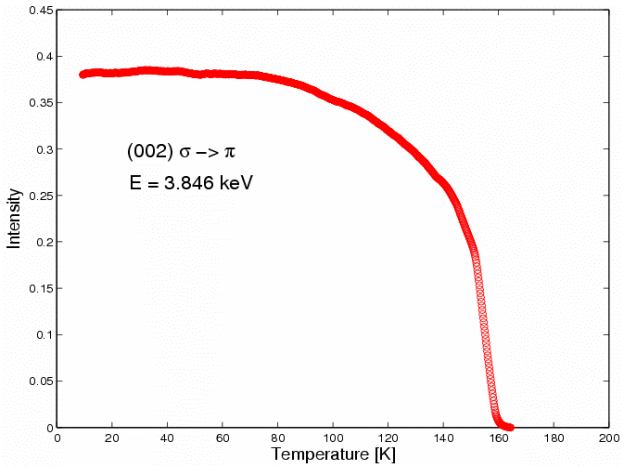

Figure 4: Temperature dependence of the resonant scattering in the channel from the ferromagnetic component. The non-resonant scattering background due to polarisation leakage from the Au (111) analyser was subtracted.

Direct Observation of large splitting in the d-band in holmium

S. D. Brown, L. Bouchenoire, P. Thompson, D. Mannix, P. Strange - for further information contact S. D. Brown at XMaS, ESRF, Grenoble 38043. sbrown@esrf.fr

The interpretation of rare-earth x-ray resonant magnetic scattering (XRMS) and x-ray magnetic circular dichroism (XMCD) at the L absorption edges and the identification of dipolar (E1) and pre-edge quadrupolar (E2) features have been controversial subjects since the first experimental results were obtained. The use of rare-earth intermetallics in high performance permanent magnets highlights the importance of the correct assignment of E1 and E2 contributions in order to describe experimental results in terms of *5d-3d* band hybridisation and *5d-4f* intra atomic exchange. Previous studies of holmium have always led to purely quadrupolar assignment of the pre-edge peak in the XRMS spectra.

Below 20 K there is a lock-in transition to a modulation wavevector of $\tau = 1/6$ and the moments tilt out of the basal plane to form a conical magnetic structure with a net ferromagnetic moment along the *c* axis. Ferromagnetic measurements were performed on XMaS, scattering horizontally from the (300) reflection through an angle of 96.1° at the L_3 edge. Asymmetry ratios were obtained through reversal of a vertical magnetic field applied along the *c* axis, provided by the 1 Tesla electromagnet, which are plotted in the middle panel of Fig 1. From the angular terms in the XRMS cross section, the quadrupole contribution is essentially zero in this configuration and we may thus conclusively assign both low and high energy peaks as dipole in origin, indicating a splitting of the d-band of 6.9 eV

In the purely antiferromagnetic phase at 40 K, the energy dependence of the (006-τ) magnetic satellite was monitored whilst scattering through an angle of 105.0°. Polarization analysis was performed in order to isolate the $\pi\rightarrow\pi$ and $\pi\rightarrow\sigma$ magnetic scattering channels. The theoretical ratio of the dipole part of these two intensities, given by the angular terms in the XRMS cross section, is 2.52. The $\pi\rightarrow\sigma$ intensity multiplied by 2.52 is plotted in the top panel of Fig. 1 along with the $\pi\rightarrow\pi$ intensity. The perfect superposition of these two spectra again demonstrates that both the low and high energy peaks are dipolar in origin.

The theoretical method used to calculate the ferromagnetic asymmetry ratio is a first principles calculation of XRMS based on standard time-dependent perturbation theory, where the scattering amplitudes are calculated to second order in the photon-electron interaction vertex. For a quantitative description of XRMS an accurate and detailed description of the electronic structure of holmium is necessary. To obtain this we have used the local spin density approximation to density functional theory with self-interaction corrections. The theory is implemented using the fully relativistic LMTO-ASA method. The resultant calculated asymmetry ratio is given in the lower panel of Fig 1. The double dipole resonance reflects both the exchange and large crystal field splitting of the *d*-band in holmium.

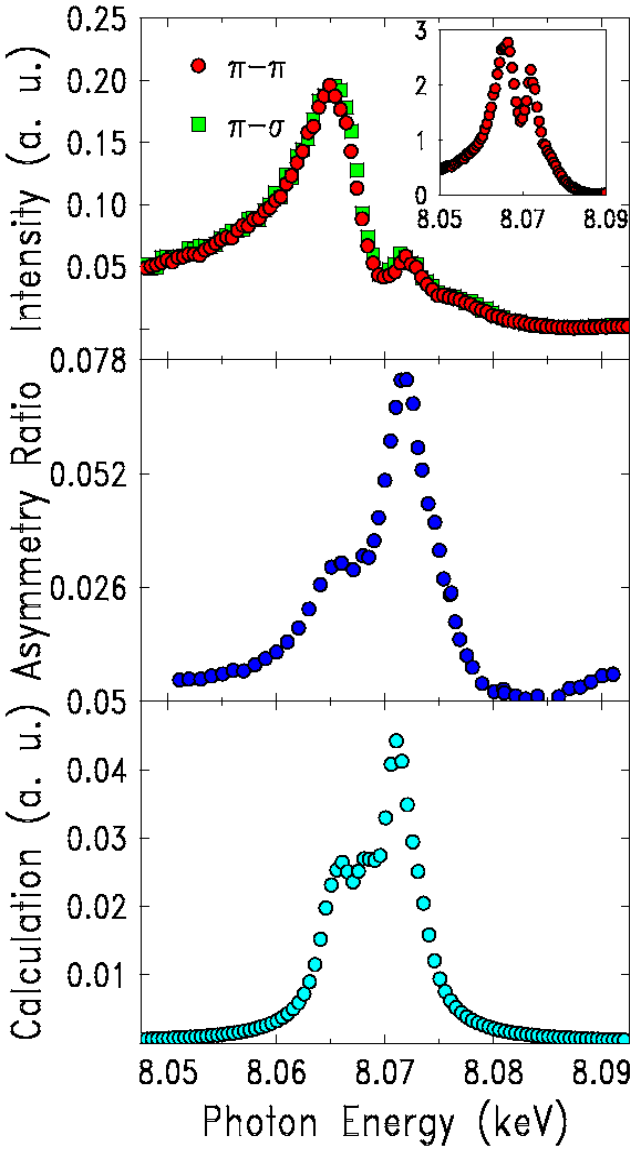

Figure 1: Top panel: Experimental antiferromagnetic $\pi\rightarrow\pi$ and $\pi\rightarrow\sigma$ intensity multiplied by 2.52. The superposition of these channels indicates the dipolar nature of both the low and high energy peaks (absorption corrected data are shown in the inset). Middle panel: Experimental ferromagnetic asymmetry ratio. Here the theoretical quadrupole contribution is virtually zero, again indicating the dipole nature of both peaks. Lower panel: The fully relativistic calculation convoluted with a 1.1 eV Guassian representing the experimental resolution.

We have shown that with the use of resonant magnetic-charge interference scattering and XRMS from ferromagnetic and antiferromagnetic moment configurations respectively, it is possible virtually to turn off the quadrupolar signal due to the respective horizontal scattering cross-sections. In the absence of a quadrupolar signal, a pre-edge resonance is observable in holmium,

which is directly assigned to be of E1 origin, This result is in excellent agreement with the fully relativistic calculation and indicates a large splitting of the *d*-band.

Charge ordering in magnetite

J.E. Lorenzo, Y. Joly, E. Nazarenko, J.L. Hodeau, C. Marin and D. Mannix - for further information contact J.E. Lorenzo at Laboratoire de Cristallographie-CNRS, F-38042 Grenoble. emelio.lorenzo@grenoble.cnrs.fr

Magnetite, Fe_3O_4, is a mixed valence ferrrimagnet that exhibits many interesting and poorly understood properties, e.g. the metal-insulator transition occurring at T_V = 120K, the so-called Verwey transition. The charge ordering pattern that magnetite displays below T_V is of great complexity and continues to challenge the scientific community. In this work we have undertaken a resonant x-ray diffraction study of the charge order in Fe_3O_4.

Two different sets of experiments were carried at BM28, with two samples from the same growth batch. Permanent magnets were attached to the sample holder that produced an average magnetic field of 0.3T at the sample and thus uniquely define the low temperature structure *c*-axis. Our diffraction results show the appearance of new reflections. Polarization analysis of the scattered beam showed that most of the intensity appears in the σσ channel. Typical raw data are shown in

Figure 1 (Upper). The spectra are dominated by the strong Fe self-absorption but nevertheless clear features, other than the absorption itself, can be seen in most measured spectra. Figure 1 (Lower) shows the near-edge region, corrected for self-absorption.

Calculations of the charge order have been performed with the program, FDMNES, and relevant results for the (4 4 1) reflection are shown in Figure 2. The calculation has been carried out for the space group *Pmca* with the atomic positions refined in. In a first step, octahedral iron atoms are supposed to have the same average charge (yellow line) and then with a charge order disproportionation (blue line). The magnitude of the charge disproportionation is calculated to be $\delta = 0.04e^-$, in contrast to the value, $\delta = 0.1e^-$ found by others. In conclusion we have shown that XRD at selected reflections exhibit very defined features, reproducible from sample to sample, that we identify with a charge ordering at the Fe on octahedral sites. Our spectra show the sought after signature of charge ordering, and calculations with FDMNES have allowed the effect to be quantified, contrary to previous work by others where no noticeable features at the edge have been reported. This small value of the charge observed in Fe_3O_4 and other compounds is of fundamental importance and strengthens the argument that covalency effects play a major role in the physics of these strongly correlated compounds.

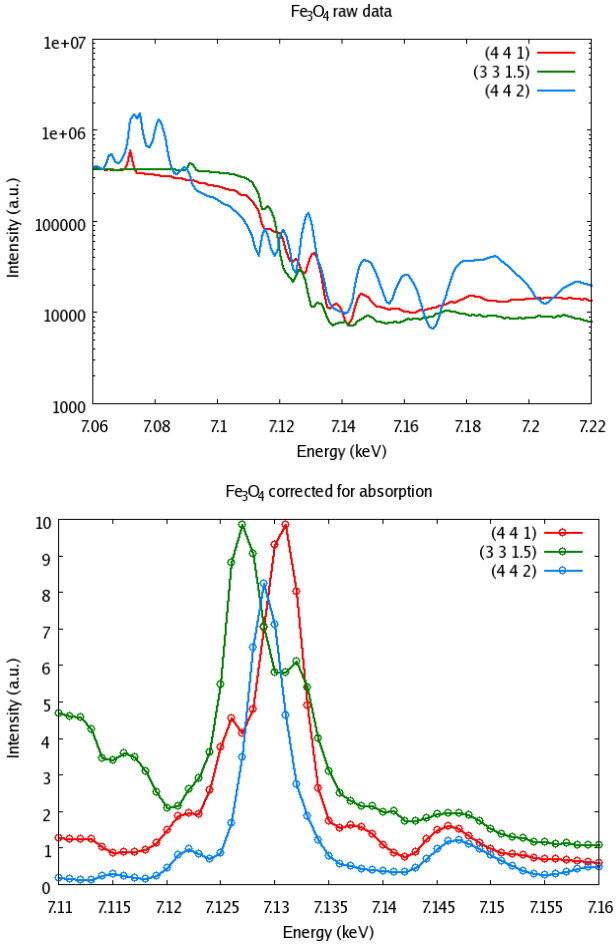

Figure 1 (Upper) Energy scans around the Fe K-edge of suitable reflections at T=50K. The log scale of the scattered intensity serves to clearly distinguish all the features occurring around the edge. After the edge, an overall decrease of the intensity by a factor of 50 has been observed that we can successfully correct. (Lower) Detail of the intensity around the edge, corrected for absorption.

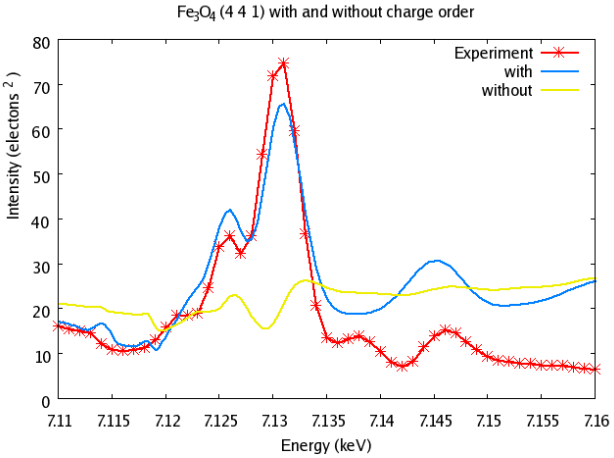

Figure 2 Calculation of the (4 4 1) reflection with and without a charge order of δ = 0.04e.

Surface Structure and Relaxation at the $Pt_3Sn(111)$/Electrolyte Interface

M. E. Gallagher, V. Stamenković, N. M. Marković and C. A. Lucas – for further information contact C. A. Lucas at Department of Physics, University of Liverpool, Liverpool clucas@liv.ac.uk

Bimetallic alloy surfaces enhance the oxidation of CO, due to a combination of bifunctional and electronic effects. The surface x-ray scattering results highlighted here represent the first ever *in-situ* characterisation of the surface structure of an alloy, under reaction conditions.

As the applied potential is cycled from the onset of hydrogen adsorption on the surface, at low potentials of E<0.2V, to the region corresponding to sulphate adsorption, 0.2<E<0.55V, there is a decrease in the intensity at (1, 0, 3.7) with a corresponding increase in the intensity at (1, 0, 4.3), shown in Figure 1(b). Such behaviour is consistent with a change in the expansion of the surface Pt and Sn atoms, which is fully reversible.

A detailed structural study by crystal truncation rod (CTR) analysis (Figure 2) shows that the surface layer of Pt and Sn atoms undergoes an expansion of ~2% of the (111) layer spacing at low potential (0.05V) in CO-free electrolyte. At 0.55V the expansion of the Pt atoms is reduced to ~0.5% and the Sn atoms are expanded by ~7%. This buckling of the surface layer is also observed in CO-saturated electrolyte and is a precursor to Sn dissolution which occurs at ~1.0V, causing irreversible roughening of the surface.

A likely cause of the increased catalytic activity, compared to Pt(111), is the oxyphillic nature of Sn. The oxidation state of Sn is determined from the near-edge energy dependence of the CTR data (Figure 3). The change in intensity at (1/2, 0, 1.9), as the incident x-ray energy is stepped through the Sn L_1 edge (4.465 keV), shows there is no shift in the edge at this position. This indicates that the surface Sn atoms are in the Sn^o state at this potential (0.05V), consistent with recent DFT calculations.

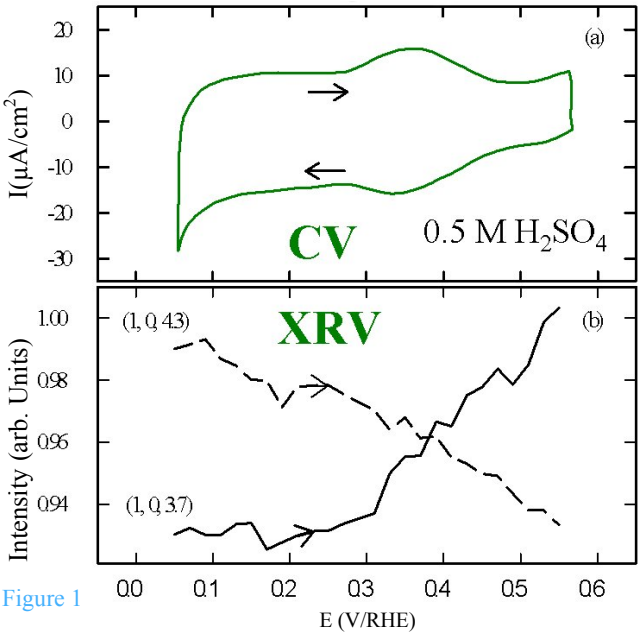

Figure 1

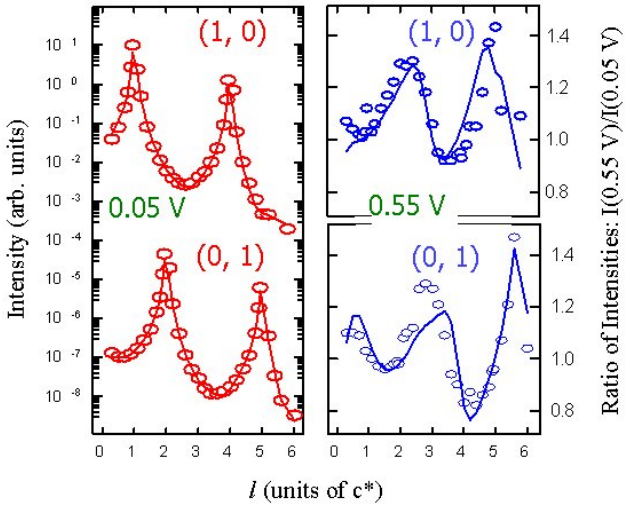

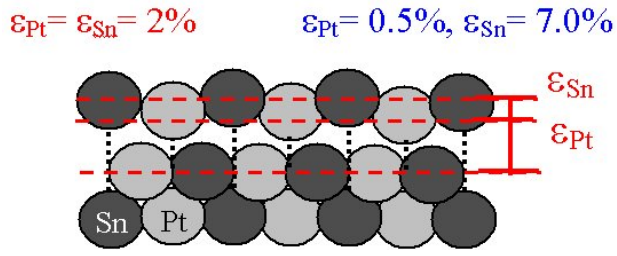

Figure 2

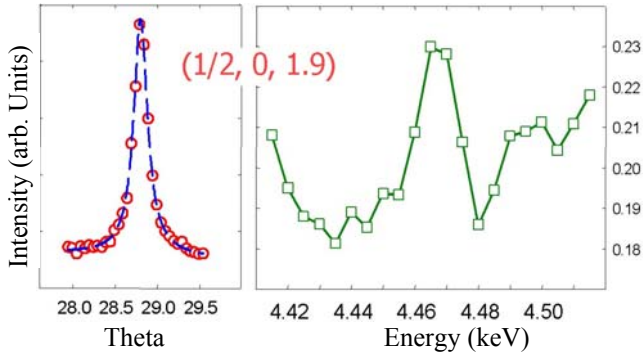

Figure 3

What use are scattered x-rays in medicine?

Richard Hugtenburg, David England and David Bradley—for further information contact: Richard Hugtenburg at School of Physics & Space Research, University of Birmingham, B15 2TT, UK r.p.hugtenburg@bham.ac.uk

Scattering processes are under-utilised as a source of information in medical imaging and in general, as scattering and fluorescence can blur the image, these processes are suppressed by careful collimation of the x-ray source and detector. Scattering methods do exist and at high angles offer an additional advantage, in particular selectivity. With collimation of the x-ray source and detector assembly, a single voxel can be analysed in a material of interest. This method is routinely exploited in x-ray fluorescence (XRF) analysis. Medical uses of XRF include measurement of the occupational uptake of heavy metal toxins and the assessment of kidney toxicity from platinum bearing chemotherapy drugs such as cisplatin and carboplatin.

Recent synchrotron based XRF analysis of trace elements in cancerous human tissue has demonstrated higher concentrations of elements such as zinc in regions that are identified as tumour. Changes in the nutrient supply can explain some of the noted increases but in the case of zinc this could be due to zinc bearing macromolecular protein, MMP-2. MMP-2, or gelatinase, has been associated with the infiltration of tumour (metastasis) into non-diseased tissue. Recent measurements of the spatial variation in zinc concentration in wax mounted tissue samples, performed using XRF analysis at XMaS, appears to support this contention suggesting that the highest concentrations of zinc occur at the interface between normal tissue and tumour with relatively small concentrations of zinc occurring in fatty tissue (see Figure 1).

The ionic state of an atom has strong bearing on the fluorescence process. A positive ionic charge increases the binding of transition metals by 10's of eV but often generating lower energy bound-state transitions with the availability of new vacancies in the valence orbital. The net effect is an increase of several eV in the energy of the absorption edge, a chemical shift, that be can used to determine the average oxidation state of a system. XANES analysis of aqueous zinc, zinc bearing tumour tissue and one other zinc bearing amorphous system, a doped sol-gel glass, show that covalently bound zinc can be detected in tumours (see Figure 2). The result further supports the contention that excess zinc in tumours is due in part to the presence of MMP-2.

XRF imaging involves the process of absorption which leads to energy deposition, i.e. a radiation dose. It is desireable to reduce radiation dose so it is would be interesting to consider whether similar information could be obtained from the anomalous variation in elastic scattering below an atomic orbital edge given that anomalous scattering is closely linked to absorption. Direct measurements of elastic scattering cross-sections have been obtained for atoms such as zinc embedded in a variety of amorphous systems, including aqueous solutions and doped sol-gel glasses. This has been carried out during recent experiments at XMaS. The experiments verify that amorphous systems provide a useful environment for testing scattering theories for isolated atoms. In turn the theories offer predictions that support the potential exploitation of the process as an imaging modality, including increased sensitivity for higher atomic number and higher charge state materials.

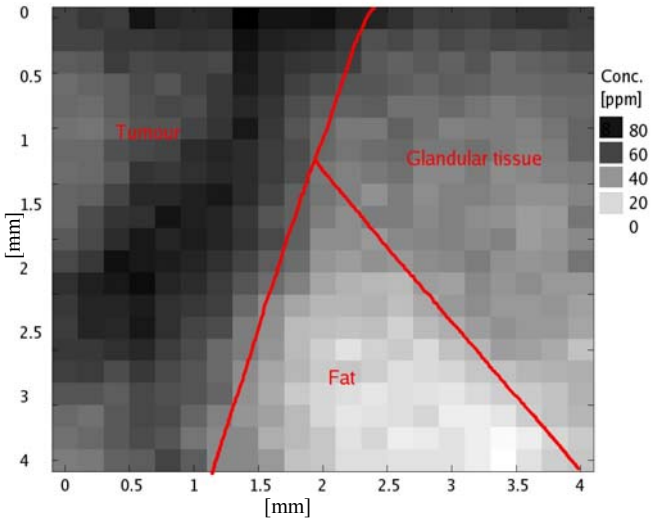

Figure 1: Distribution of Zn in a 4 mm × 4 mm section of wax mounted malignant tumour bearing tissue demonstrating Zn concentrations in the range 20-80 ppm (by wt)

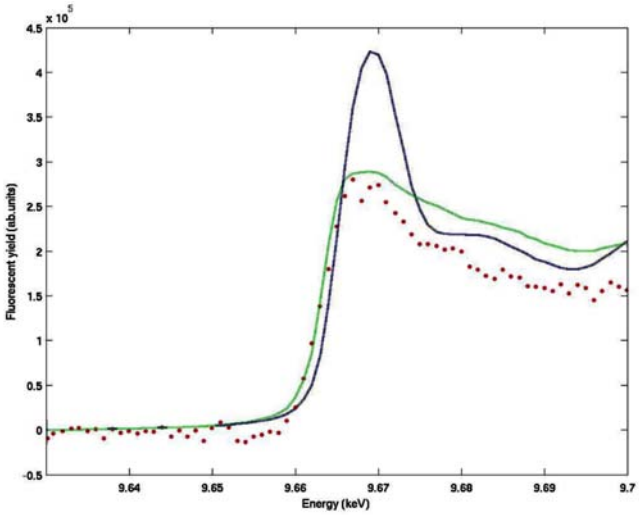

Figure 2: XANES spectra of diseased tissue (red points) versus aqueous Zn (blue line) and Zn doped glass (green line)

Orbital Stripes in Layered Manganites

T.A.W. Beale, T.R. Jestico, P.D. Hatton, S.B. Wilkins, S.D. Brown, D. Prabhakaran and A.T. Boothroyd - for further information contact Peter Hatton at Dept. of Physics, University of Durham, DH1 3LE, U.K. p.d.hatton@dur.ac.uk

In this article we present the results of *K* edge energy x-ray diffraction of $La_{2-2x}Sr_{1-2x}Mn_2O_7$ for $x = 0.6$. The azimuthal dependence of the Stokes parameter was calculated, based on an orbital model in turn predicted from a shift in wavevector of the Jahn-Teller distortion previously observed with high energy x-ray diffraction. Using *K* edge diffraction, an orbital order peak was observed around the (0 0 10) Bragg peak, where there was an absence of a Jahn-Teller signal. This peak was observed to resonate in both σ-σ and σ-π channels. The azimuthal angle dependence of these channels were measured, and agreed with the simulation calculated for the predicted orbital model.

Previous results from high energy scattering on the $x = 0.6$ bilayer have shown a shift in wave vector of the Jahn-Teller distortion peak. This shift from (h±0.25, k±0.25, l) for x = 0.5 doping to ~(h±0.2, h±0.2, l) for $x = 0.6$ doping suggests a change in the periodicity of the Jahn-Teller distortion and corresponding orbital ordering. A model was constructed forming 'quasi-stripe' ordering, with an orbital order unit cell five times larger than the chemical unit cell (Figure 1).

X-ray scattering was performed on the XMaS beamline with an incident beam energy of 6.555 keV corresponding to the Mn *K* edge. Superlattice peaks were found around the (0 0 10) Bragg peak at (h±δ, k±δ,10) where δ = 0.217. These peaks were observed in both the σ-σ and σ-π channels 90° out of phase in azimuth. Resonant enhancements in both channels (Figure 2) suggest that the peak is due to an orbital order induced splitting of the 4*p* energy level rather than a Jahn-Teller type structural distortion.

A simulation of the azimuthal dependence of the orbital ordering was calculated form geometrical considerations. This is compared with experimental data in the form of the Stokes parameter defined by

$$P = \frac{I_{\sigma\sigma} - I_{\sigma\pi}}{I_{\sigma\sigma} + I_{\sigma\pi}}$$

Figure 3 shows good agreement between the predicted model and the experimental data confirming the presence of orbital stripes.

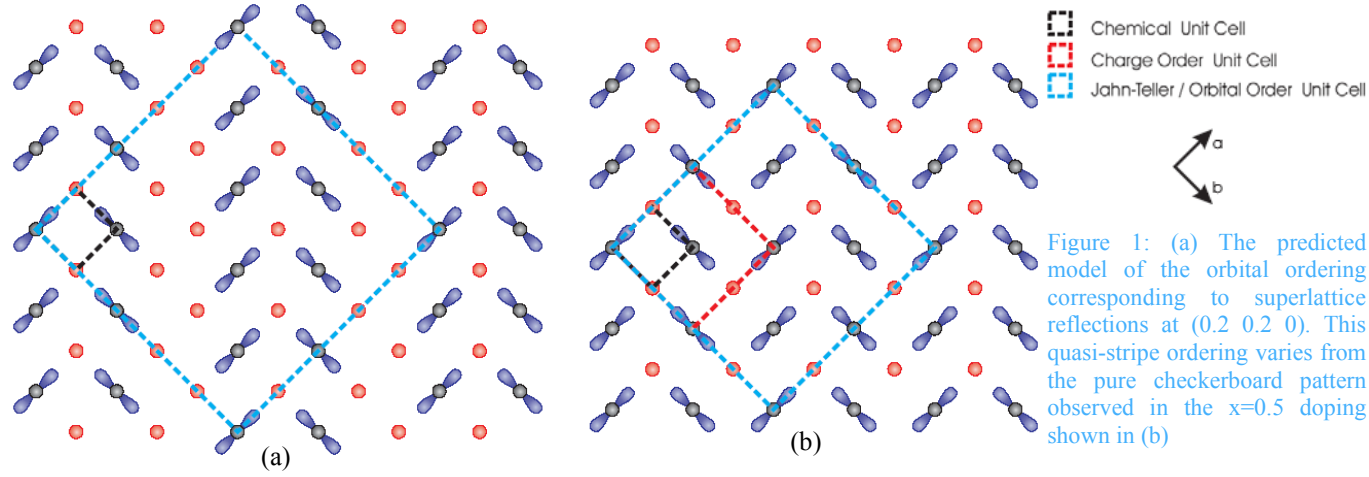

Figure 1: (a) The predicted model of the orbital ordering corresponding to superlattice reflections at (0.2 0.2 0). This quasi-stripe ordering varies from the pure checkerboard pattern observed in the x=0.5 doping shown in (b)

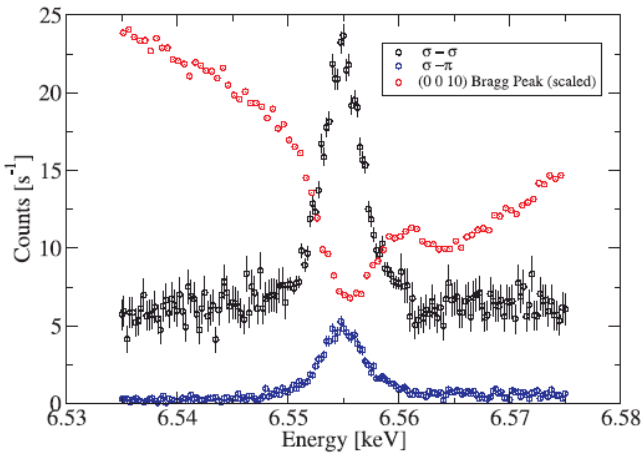

Figure 2: Energy dependence of the (δ,δ, 10) peak in the σ-σ and σ-π channels. The manganese K edge absorption of the (0 0 10) Bragg peak is shown for comparison.

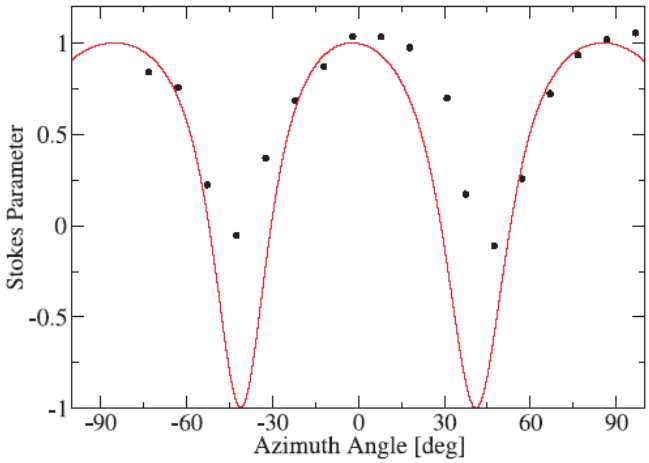

Figure 3: Calculated and experimental data for the Stokes parameters at (δ,δ, 10).

Resonant Ferromagnetic Diffraction from Uranium Sulphide

L Bouchenoire, S D Brown, S P Collins, P Thompson, D Mannix and D Laundy—for further information contact S D Brown at XMaS, BM28, ESRF boucheno@esrf.fr

While resonant magnetic diffraction has been extensively employed to study antiferromagnetic actinides, very little work has been done on ferromagnetic samples, where the strong charge and the weak magnetic peaks coincide in reciprocal space. The induced sulphur ferromagnetic moment in US was studied for the first time at the sulphur K edge (2.472 keV) on XMaS using resonant magnetic-charge interference scattering. This commissioning experiment was made possible following a modification to the metal support of the monochromator first crystal reported elsewhere in this Newsletter.

This experiment was performed in a horizontal scattering geometry with the 2q angle of the (002) reflection close to 132°. The magnetic field was applied in the vertical direction. Asymmetry ratios of up to 2.5 % were measured with a field of ±0.28 T at 100 K as shown in Figure 1. As a comparison, the flipping ratio is about 90% at the U M_4 edge (see XMaS Newsletter 2002). The flipping ratio was also studied as a function of temperature across the Curie temperature (180 K) as shown in Figure 2, in order to determine the value of the critical exponent, β, which describes the power-law temperature dependence of the sample's magnetisation. Mean field theory predicts that $\tilde{\beta}=2\beta$, where $\tilde{\beta}$ describes the power-law temperature dependence of the lattice strain. Whereas bulk magnetic measurements are in agreement with theory, previous x-ray results have found that $\tilde{\beta}$ is half the expected value. Temperature and field dependence measurements of the (002) reflection were also performed at the U M_4 edge. These combined data sets should help to evaluate the value of β accurately and determine whether the uranium M edge and sulphur K edge data are in agreement. The critical exponent, $\tilde{\beta}$, will be extracted from the temperature dependence of the (111) peak splitting carried out with no field. This study should thereby clarify the discrepancy between magnetic and structural analysis. The anomaly in the flipping ratio (see Figure 2) between 130K and 140K appears to be statistically significant and will be studied further.

During this period of in-house time, we also had to overcome problems with low detectors efficiency and strong air absorption at the S edge. The Bicron detector was found to be unusable and a solid state detector was employed instead. A special shroud had to be manufactured for this geometry so that there was no air gap between the incident beam and the detector. However, we have demonstrated that both charge and magnetic scattering experiments can be carried out at the sulphur K edge on XMaS, providing a valuable new facility on XMaS.

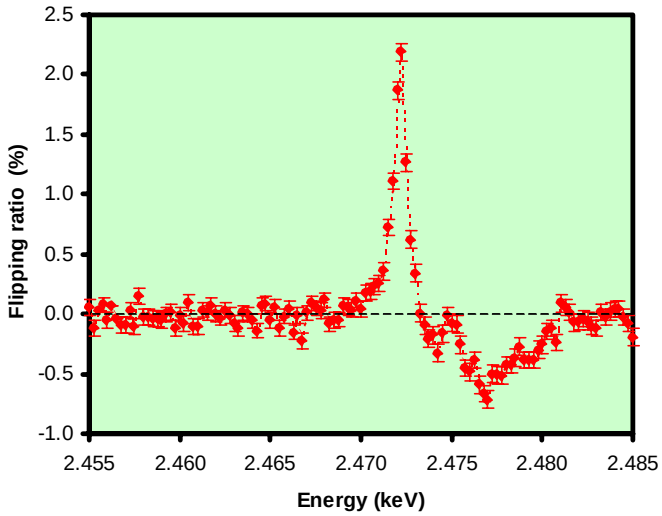

Figure 1: Asymmetry ratio measured at 100°K across the S edge.

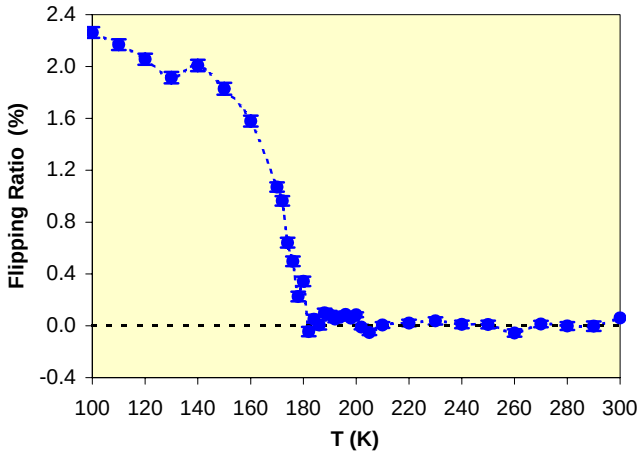

Figure 2: Asymmetry ratio measured at the S edge across Tc (180°K).

Please note—The experimental reports in the previous pages are all as yet unpublished. Please email the contact person if you are interested in any of them or wish to quote these results elsewhere.

Our web site

This is at:

http://www.esrf.fr/UsersAndScience/Experiments/CRG/BM28/

It contains the definitive information about the beamline and an on-line beamline manual.

Living allowances

These are still 55 euros per day per beamline user—the equivalent actually reimbursed in pounds sterling, of course. XMaS will continue to support up to 4 users per experiment if you can make a case for the presence of the fourth experimentalist. The ESRF hostel still appears adequate to accommodate all our users, though CRG users will always have a lower priority than the ESRF's own users. Do remember to complete the web-based "A form" requested of you when you receive the ESRF invitation, all attendees must be listed, since this informs the safety group of the attendees and is used to organise all site passes, meal cards and accommodation.

Beamline people

There have been no changes in the beamline staff since the last Newsletter.

Project Co-ordinator - David Paul, (dpaul@esrf.fr), is the person who can provide you with general information about the beamline, application procedures etc. David should normally be your first point of contact.

Beamline Scientists - Simon Brown (sbrown@esrf.fr), Danny Mannix (danny@esrf.fr) and Laurence Bouchenoire (boucheno@esrf.fr) continue as beamline scientists.

Technical Support – Paul Thompson (thompso@esrf.fr) continues to work on instrument development and provides technical support for the beamline. John Kervin (jkervin@liv.ac.uk), who is based at Liverpool University, provides further technical back-up and spends part of his time on-site at XMaS.

Project Directors — Malcolm Cooper (m.j.cooper@warwick.ac.uk) and Chris Lucas (clucas@liv.ac.uk) continue to travel between the UK and France to oversee the operation of the beamline. The administration for XMaS continues to be handled by Sandra Beaufoy at Warwick University (s.beaufoy@.warwick.ac.uk).

The Project Management Committee

The current membership of the committee is as follows:
Denis Greig (chair)
Des McMorrow
Peter Hatton
Jose Baruchel
Bob Cernik
Simon Crook
Meeting twice a year, in addition to the above, the directors, the chair of the PRP and beamline team are in attendance.

The Peer Review Panel

The current membership of the panel is as follows:
Sean Langridge (chair)
Paul Strange
Paul Fewster
Nick Brookes
Steve Collins
Richard Jones
In addition either Malcolm Cooper or Chris Lucas attend their meetings.

Housekeeping!!

We take some trouble to keep the beamline clean and tidy, please leave the beamline in the same state! At the end of your experiment samples should be removed from cryostat and other sample environment mounts, tools, etc returned to racks and unwanted materials disposed of in an appropriate manner. When travel arrangements are made, therefore, please allow additional time, at the cessation of beam, to effect a tidy-up.

PUBLISH PLEASE!!……..and keep us informed

Although our list of papers reporting work on XMaS is growing we still need more of those publications to appear. We ask you to provide Sandra Beaufoy not only with the reference but also a preprint/reprint for our growing collection. Note that the abstract of a publication can also serve as the experimental report!

IMPORTANT!

When beamline staff have made a significant contribution to your scientific investigation you may naturally want to include them as authors. Otherwise we ask that you add an acknowledgement, of the form:

"This work was performed on the EPSRC-funded XMaS beam line at the ESRF, directed by M.J. Cooper and C.A. Lucas. We are grateful to the beam line team of S.D. Brown, D.F. Paul, D. Mannix, L. Bouchenoire and P. Thompson for their invaluable assistance, and to S. Beaufoy and J. Kervin for additional support."

Guidelines for Applying for Beam-time at the XMaS beamline

XMaS Pluo B3, ESRF, BP 220, 38043 Grenoble Cedex, France
Tel: +33 (0)4 76 88 24 36 Fax: +33 (0)4 76 88 24 55
web page : http://www.esrf.fr/exp_facilities/BM28/xmas.html email: dpaul@esrf.fr

Beamline Operation

The XMaS beamline at the ESRF, which came into operation in April 1998, has some 133 days of beam time available each year for UK user experiments, after deducting time allocated for ESRF users, machine dedicated runs and maintenance days. During the year, two long shut-downs of the ESRF are planned: 5 weeks in winter and 4 weeks in summer. At the ESRF beam is available for user experiments 24 hours a day.

Applications for Beam Time

Two proposal review rounds are held each year, with deadlines for submission of applications, normally, the end of **March** and **September** for the scheduling periods August to end of February, and March to July, respectively. **Applications for Beam Time** are to be submitted **electronically** (the paper versions are not acceptable) following the successful model used by the ESRF and ourselves. Please consult the instructions given in the ESRF web page:

www.esrf.fr

Follow the links: "**User Guide**"
And: "**Applying for Beam Time**"

Follow the instructions carefully — you must choose "XMAS-BM28" and "CRG Proposal" at the appropriate stage in the process. A detailed description of the process is always included in the reminder that is emailed to our users shortly before the deadline — for any problems contact D. Paul, as above.

Technical specifications of the Beamline and instrumentation available are described in the *XMaS* web page.
When preparing your application, please consider the following:

- All sections of the form must be filled in. Particular attention should be given to the safety aspects, and the name and characteristics of the substance completed carefully. Experimental conditions requiring special safety precautions such as the use of lasers, high pressure cells, dangerous substances, toxic substances and radioactive materials, must be clearly stated in the proposal. Moreover, any ancillary equipment supplied by the user must conform with the appropriate French regulations. Further information may be obtained from the ESRF Experimental Safety Officer, tel: +33 (0)4 76 88 23 69; fax: +33 (0)4 76 88 24 18.
- Please indicate your date preferences, including any dates that you would be unable to attend if invited for an experiment. This will help us to produce a schedule that is satisfactory for all.
- An experimental report on previous measurements must be submitted. New applications will not be considered unless a report on previous work is submitted. These also should be submitted electronically, following the ESRF model. The procedure for the submission follows that for the submission of proposals — again, follow the instructions in the ESRF's web pages carefully. Reports must be submitted within 6 months of the experiment.
- The XMaS beamline is available for one third of its operational time to the ESRF's user community. Applications for beamtime within that quota should be made in the ESRF's proposal round - **Note: their deadlines are earlier than for XMaS! - 1st March and 1st September.** Applications for the same experiment may be made both to XMaS directly and to the ESRF. Obviously proposals successfully awarded beamtime by the ESRF will not then be given beamtime additionally in the XMaS allocation.

Assessment of Applications

The Peer Review Panel for the UK-CRG considers the proposals, grades them according to scientific excellence, adjusts the requested beam time if required, and recommends proposals to be allocated beam time on the beamline.
Proposals which are allocated beam time must in addition meet ESRF safety and XMaS technical feasibility requirements.
Following each meeting of the Peer Review Panel, proposers will be informed of the decisions taken and some feedback provided.

THE UNIVERSITY of LIVERPOOL

is an EPSRC sponsored project

THE UNIVERSITY OF WARWICK